TEMPERATURE EFFECT EVALUATION OF FML PANELS UNDER QUASI-STATIC INDENTATION LOADING

Z.P. Chow*,Z. Ahmad*,K.J. Wong

Faculty of Mechanical Engineering, Universiti Teknologi Malaysia, 81310 Johor Bahru, Malaysia
*For correspondence; Tel. + (60) 163026502, E-mail: zhenpei.chow@gmail.com
*For correspondence; Tel. + (60) 75557048, E-mail: azaini@mail.fkm.utm.my

ABSTRACT: *The main goal of this study is to characterize and develop use of fiber metal laminates (FML) panels at elevated temperature. The effect of elevated temperature on FML panels under quasi-static indentation was investigated at 30°C, 70°C and 110°C. The FML panel used here is GLARE 3-3/2 comprising of three layers of Aluminum 2024-T3 alternatingly sandwiching two layers of cross-plied unidirectional glass fiber reinforced polymer (GFRP). Quasi-static indentation test was conducted with hemispherical indenter at a rate of 1 mm/min on GLARE-3/2 panels using Shimadzu universal testing machine within a controlled heating chamber. Performance and response were evaluated by examining load-displacement curves, peak load and total energy absorption. Afterwards, temperature dependent empirical models are used to capture and predict indentation property across the range of temperature. It was observed that increasing temperature causes slightly larger global bending but subsequently lower local perforation resistance to deformation. By comparing the curve fitted trend of peak load and total energy absorption, GLARE-3/2 showed negligible reduction in peak load at 70°C followed by more significant reduction at 110°C. In contrary, energy absorption versus temperature follows a marginal decline at 70°C yet smaller decrease at 110°C. Conclusively, increased temperatures cause significant but not severe drop of indentation resistance and energy absorption of FML.*

Keywords: Temperature, Quasi-static indentation, Fiber metal laminates, GLARE

1. INTRODUCTION

Fiber metal laminates (FML) comprises of alternating layers of bonded aluminum and fiber reinforced composite with superior impact, fatigue and corrosion resistance compared monolithic aluminum or composites [1, 2]. The alternating layering of composite laminates acts as fiber bridging that greatly reduces crack propagation while presence of aluminum helps in absorbing impact energy and improves damage visibility [3, 4].

The superior impact and damage capabilities of FML draw attention of numerous studies and research on the indentation, low-velocity and ballistic impact of FML, ranging from a wide variety of different materials, thickness, orientation and compositions [3, 5]. In more recent study, Jaroslaw et al. [6] investigated the differential impact resistance between carbon and glass based fiber aluminum laminates under low velocity. They found higher damage resistance in glass FML due to energy absorbed through delamination and plastic deformation, while perforation governs energy absorption in carbon FML. In an analysis of aramid based fiber metal laminate, Gonzalez-Canche et al. [7] found excellent strain to failure governed by global plastic deformation can be obtained by superior adhesion between the layers. A.P. Sharma et al. [8] studied the effects of reducing aluminum thickness while distributing it throughout the FML that is effective in decreasing peak load but elevated the extent of damage.

Due to separate entities of laminates, FML has potential to become thermal barriers and to be used at different temperatures [9, 10]. This draws attention to FML response towards indentation and impact damage resistance at different temperature ranges [11, 12]. For instance, impact response of GFRP by Badawy [13] found that GFRP's resistance towards impact at different temperatures depend on fiber volume fraction and exposure time. Study by Hu et al. [14] shows that tensile strength and interlaminar shear strength of FML are reduced by almost half at 220°C. Comparison between glass, carbon and hybrid based fibers by Hawileh et al. [15] found that tensile strength of glass fibers are the least affected by temperature effect. Jakubczak and Bienias [16] compared the quasi-static indentation and dynamic load between glass and carbon based FML. Such study reported that the peak load and deformation between quasi-static and dynamic tests of Al/GFRP are almost identical, indicating the usefulness of analyzing quasi-static indentation.

In 2001, Mahieux et al. [17] published modeling technique of material properties for polymer type composites. Gibson et al. [18] developed a method with help of laminate theory to estimate high temperature effects on composites. A detailed analysis between material degradation empirical models was reported by Correia et al. [19] where Gompertz function model proved useful in capturing mechanical properties degradation of GFRP. There have been no open literature found on the quasi-static indentation behavior of FML plates. Moreover, no modeling methods have been carried out on predicting the temperature dependence of indentation properties.

The main aim of this paper is to characterize and evaluates the quasi-static indentation response of GLARE 3-3/2 FML panels under elevated temperature. Aluminum 2024-T3 cross plied with S2-grade GFRP are foremost fabricated into square plates. Quasi-static indentation tests were conducted on the panels at 30°C, 70°C and 110°C that are clamped between plates with circular opening. Tests are performed well within the range within the glass transition temperature, T_g where the material behavior of the GFRP remains in its glassy state. The load-displacement curves were then extracted from the testing machine and analyzed. Empirical models from literature are used to capture the impact resistance degradation trends of peak load and total energy absorbed with respect to temperature. Assessments are carried out to determine viability and accuracy of each model in estimating FML response across elevated temperature.

2.   EXPERIMENTAL DETAILS

The specimens are fabricated according to commercial type FML Glare 3-3/2 with layup of [A/0/90/A/90/0/A]. The laminate consists of three aluminium layers sandwiching two layers of 0°/90° GFRP. The FML panels have a square dimension of 200 x 200 mm. The Aluminium 2024-T3 and unidirectional S2-type fibre GFRP sheets are supplied from X-Plas Singapore. Aluminium 2024-T3 sheets each have a thickness of 0.4 mm. The sheets are first sand-blasted under grid 150, followed by sulphuric acid anodizing with gloss finish. GFRP panels consist of lay up of glass fibre prepregs with pre-impregnated epoxy resin with a T_g of 125°C. Each prepreg has a nominal fiber volume content of 0.5 with a thickness of 0.15 mm. The individual prepreg ply is first cured using hot press, and then allowed for binding within hot oven at 120°C.

Aluminium and GFRP panels are bonded together using ProAssure Wrap epoxy resin with glass transition temperature of 130°C that is supplied from IO Setia Ventures. Before bonding, all the surfaces are lightly treated with Acetone to remove traces of dust, oil and fingerprints. The specimens are sandwiched together using hand layup method and left for 4 days at room temperature to fully cure. The total thickness of the Glare plate is approximately 1.8 mm. A total of 9 specimens are prepared.

Specimens were tested using universal testing machine Shimadzu AG-X plus 100 kN machine with analysis using Trapezium X. To achieve constant steady temperature of 30°C, 70°C and 110°C, built in thermostatic chamber of the machine, TCE-N300 is used. The range of temperature applied is kept within the boundary of the T_g In terms of fixture, two 150 mm x 150 mm mild steel plates with a circular opening of diameter 127 mm are used to clamp the panels during the test setup. A stainless steel cylindrical rod with hemispherical end of 12.7 mm diameter is used as an indenter to carry out the quasi-static indentation. The setup is shown in Fig. 1. The rate of testing is set to a quasi-static rate of 1 mm/min to minimize any strain rate effect and minimize data scattering. Three specimens are used for each temperature. Load-displacement results of each temperature are compared.
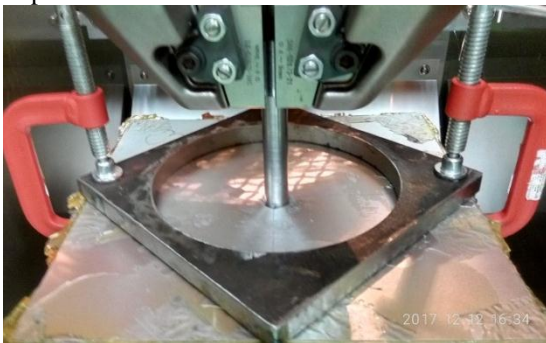

Fig (1): Quasi-static indentation specimen test setup

3.   EXPERIMENTAL RESULTS

Fig. 2 shows the load vs. displacement histories that are obtained from the corresponding temperature of 30°C, 70°C and 110°C respectively. For all three temperatures, a good repeatability is observed. By analysing the load-displacement

curves, the different stages of the indentation through the FML panel can be deduced and differences at each temperature can be explained. Generally, the all three curve profiles can be characterized into several stages which follow similar trend, as shown in Fig. 2. The load profile starts by increasing with a constant gradient until it enters brief cycles of ascending step profile. Then the trend reverts back to constant load increase until maximum load. After the maximum load, the load declines in a constant rate until it reaches descending step profile again. Finally, the load enters a plateau region which marks the end of the deformation.
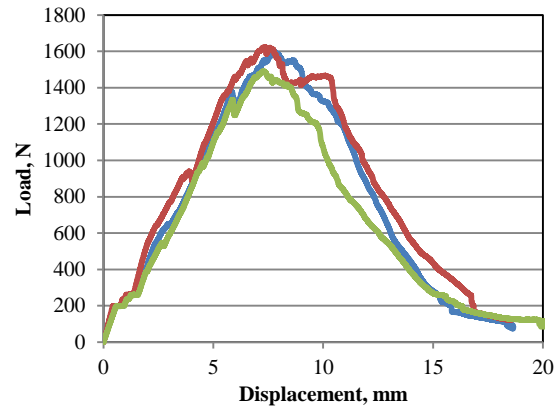
(a)
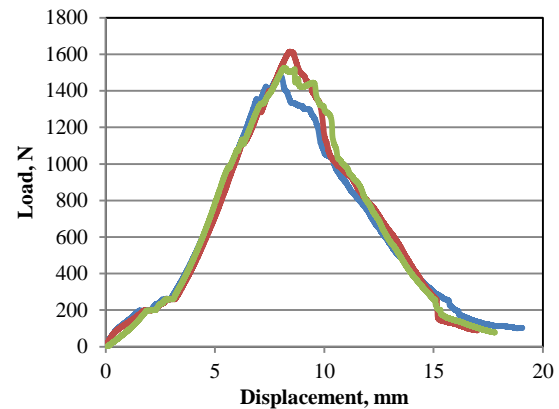
(b)
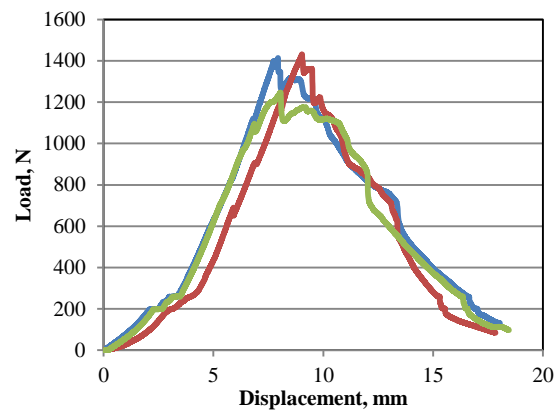
(c)

Fig (2): Load vs. displacement curve of quasi-static indentation test at (a) 30°C, (b) 70°C and (c) 110°C.

Stage one of indentation is governed by smooth climbing of the profile which marks the global bending of the entire FML

panel through the circular opening which is purely elastic. For all three temperatures, the first stage reaches similar load of 200 N. However, the displacement stretches with increasing temperature, indicating reduced stiffness of the entire FML structure.

After the global bending, stage two is the brief cycles of ascending step profile. The steps represent compression of each layer to reach stabilization of contact between the indenter and each layer of the FML. Similar to the global bending at first stage, the load increment of stage two is constant under effect of temperature, but a drop of stiffness stretches the displacement with respect to temperature.

The third stage marks the initiation of internal damage such as delamination between the aluminium and GFRP layers, matrix cracking and fibre breakage of GFRP and aluminium layer plastic deformation. There is evidently more load fluctuations for 30°C during the stage three due to unstable damage propagation across the internal structure. Fluctuations are very limited for 70°C and 110°C due to much stable and smooth internal damage initiation across the layers attributed to heat. Onset the peak load, the stiffness loss causes decrease of gradient for 30°C, but this does not occur for elevated temperatures.

As reaching the peak load, the plastic deformation caused by internal damage exceeds the threshold stress value; the first crack occurs on the top layer, leading to the drop of load. Subsequent layers also reach maximum stress straight after and develop cracks. It is noted that after the peak load, it drops gradually for 30°C, while load drops more rapidly for 70°C and 110°C. Indenter cracks and perforates the layers with less displacement at higher temperatures due to lower laminate resistance to perforation with weaker delamination resistance and GFRP strength.

As each layer cracks and the material fails, the load drops until around 200 N where it undergoes brief decreasing step profile. The step drop is similar to stage one of the curves. In this case, each step is indication of the indenter puncturing each layer. Finally the load reaches a plateau. The load does not drop to zero, due to friction contact between the indenter and the punctured hole.

Table 1 shows average value of the peak load and total energy absorbed at each temperature with standard deviation errors analyzed from Fig 2. The peak load drops slightly from 30°C (1569.49 N) to 70°C (1538.55 N) with only a loss of 1.97%. At 110°C, the peak load declines more significantly by 13.1% to 1363.82 N. However, in terms of total energy absorbed, the drop from 30°C (14.42 N) to 70°C (11.59 N) is much more prevalent with 19.63%. The difference increases slightly more which is up to 26.49% at 110°C (10.60 N).

Table (1) Peak load and total energy absorbed at each temperature (with standard deviation).

Temperature	30°C	70°C	110°C
Peak Load, N	1569.46 ±40.58	1538.55 ±40.34	1363.82 ±58.91
Total Energy Absorbed, J	14.42 ±0.75	11.59 ±0.05	10.60 ±0.42

4. TEMPERATURE DEPENDENT PROPERTY MODELING

To analyze the indentation performance of the FML panels across temperatures of 30°C to 110°C, the use of empirical models is required to capture trend of degradation of resistance towards indentation. Several existing proposed models used to predict mechanical properties degradation of composites due to temperature has been found to be suitable. The following models by Mahieux et al. [17], Gibson et al. [18] and Correia et al. [19] are originally used for mechanical properties degradation of pure composite structure due to temperature. In this case, they are altered to model trend of indentation properties, P of FML against temperature, T.

Mahieux et al. [17] developed a model for modulus of polymers versus temperature based on Weibull's equation:

$$P(T) = P_{max} + (P_{min} - P_{max}) \times exp\left[-\left(\frac{T}{T_0}\right)^m\right] \quad (1)$$

where P_{max} is property at maximum temperature, P_{min} is the property at minimum temperature, T_0 and m are parameters to be curve fitted.

A model utilizing laminate theory which effectively captures compressive behavior by Gibson et al. [18]:

$$P(T) = P_{min} - \frac{P_{min} - P_{max}}{2} \times \left(1 + \tanh\left[k'^{(T-T_x)}\right]\right) \quad (2)$$

where k' and T_x are the fitting parameters.

Based on Gompertz statistical distribution, Correia et al. [19] proposed a model that is well suited in predicting degradation of shear and compressive strengths of GFRP as follows:

$$P(T) = \left(1 - e^{B \cdot e^{C \times T}}\right) \times (P_{min} - P_{max}) + P_{max} \quad (3)$$

where B and C are the constant parameters to be curve fitted. The residual property model by Wong [20] was originally used for the degradation of composite materials due to moisture. In this case, their model is suitable to capture the degradation pattern of the current study.

$$P(T) = 1 - \left(1 - \frac{P_{max}}{P_{min}}\right) \cdot \left(\frac{T - T_{min}}{T_{max} - T_{min}}\right)^\zeta \quad (4)$$

where T_{min} is the minimum temperature, T_{max} is the maximum temperature, ζ is the only singular parameter to be fitted.

5. MODELING DISCUSSION

The experimental data extracted from Section 3 is used as data for curve fitting, with the temperature range from 30°C to 110°C. The temperature dependent modeling curves is then used to plot normalized peak load and normalized total energy absorbed versus temperature as shown in Fig. 3.
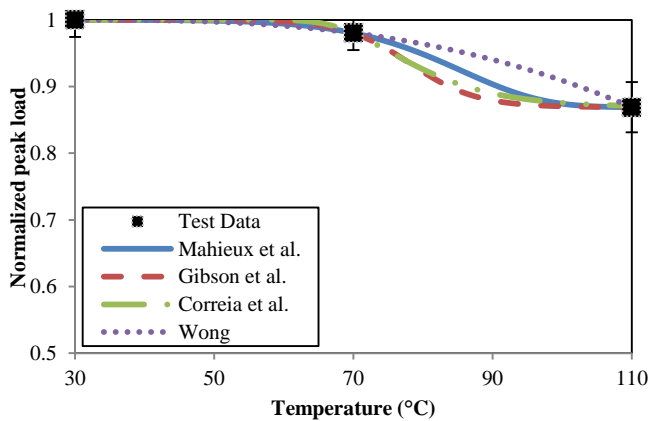
For the first 3 models, the values of temperature are foremost normalized to facilitate curve fitting and obtain each parameters, then converted back into temperature value for the figures. For the model by Wong [20], the temperature is already defined by means of homologous method, therefore no normalizing is necessary.

For Fig. 3(a), all models are able to plot the normalized peak load versus temperature with good representation. However, for this case of only 3 test data points, the model by Wong [20] is more straightforward from 70°C to 110°C onwards in describing the initial gradual reduction follow by increasing steepness. The differences between the models are further
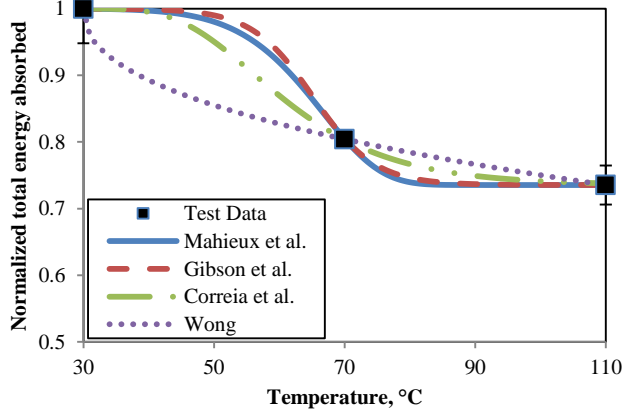
exemplified for normalized total energy absorbed versus temperature in Fig. 3(b). The models by Mahieux et al., Gibson et al. and Correia et al. [17-19] fitted the overall trend as a 'z' profile. The curve initially falls steadily, increasing in slope until a relatively steep decline at 70°C, and becomes a plateau upon reaching 90°C onwards. On the other hand, model by Wong [20] predicts initial drop of total energy absorbed with steep slope, that gradually becomes smaller in slope until 110°C.

Hence, the model adopted from Wong [20] is more suitable for the range of this study, as it is more easily fitted, with the highest R-squared value. The Wong's model describes and portray the behavior and trend of both properties in a more direct and accurate manner. Moreover, the model only requires fitting one singular parameter unlike two parameters required by the other models.

The values of fitting parameters for all the models are compiled in Table 2. From the model by Wong, the parameter ζ for peak load (2.732) describes an initially stable, followed by more and more drastic decrease towards the maximum temperature. This behavior indicates stable peak load at low temperature range. On the other hand, ζ of total energy absorption (0.434) means the property decreases drastically even from minimum temperature, indicating that the energy absorption of the FML plates is very sensitive to temperature.

Table (2) Normalized parameters of peak load and total energy absorbed curve fitted at each temperature.

Model	Property	Peak load	Total energy absorbed
Mahieux et al. (2001)	T_0,°C	2.898	2.254
	m	8.35	8.459
Gibson et al. (2006)	$T_{g\text{-}mech}$,°C	2.605	2.172
	k'	3.134	3.188
Correia et al. (2013)	B	-8019	-124.6
	C	-3.583	-2.586
Wong (2013)	ζ	2.732	0.434

6.   CONCLUSIONS

This study analyzed and compared the quasi-static indentation of FML Glare 3-3/2 panels experimentally under temperatures of 30°C, 70°C and 110°C. Empirical models adopted from literature are used to capture and characterize the trend of peak load and total energy absorption. A temperature dependent property model with the best suitability is chosen. The conclusion can be summarized as follows.

1. Medium temperature of 70°C decreases the peak load of the FML only slightly by 1.97% but marginally decreases the total energy absorption by 19.63%.
2. High temperature of 110°C causes larger degree of decline in the peak load to 13.1% but only slightly adds the decrease of total energy absorption to 26.49%.
3. Elevated temperature causes significant yet not severe degradation of the energy absorption capability of Glare FMLs. The degree of degradation at 70°C to 110°C has no drastic difference (only from 19.63% to 26.49%).
4. Wong's model which was originally used for the moisture degradation of the composites is more preferable compared to the rest of the models. The model showed good fitting capabilities as well as ability to describe the trend accurately. However, since this study only has three temperature data points across the range of 30°C to 110°C, it is recommended that a more in depth study with five or more points of temperature across this range or a larger range can be conducted in the future to testify the model used herein.

Fig (3) (a) Normalized peak load vs. temperature
(b) Total energy absorbed vs. temperature.

7.   ACKNOWLEDGEMENTS

8.   REFERENCE

[1]   Roebroeks, G.H.J.J., *Fibre-metal laminates: Recent developments and applications.* International Journal of Fatigue, 1994. **16**(1): p. 33-42.

[2]   Vlot, A., J.W. Gunnink, and SpringerLink (Online service), *Fibre Metal Laminates An Introduction.* 2001, Springer Netherlands,: Dordrecht. p. 1 online resource.

[3] Chai, G.B. and P. Manikandan, *Low velocity impact response of fibre-metal laminates – A review.* Composite Structures, 2014. **107**: p. 363-381.

[4] Vlot, A., *Impact properties of Fibre Metal Laminates.* Composites Engineering, 1993. **3**(10): p. 911-927.

[5] Sadighi, M., R.C. Alderliesten, and R. Benedictus, *Impact resistance of fiber-metal laminates: A review.* International Journal of Impact Engineering, 2012. **49**: p. 77-90.

[6] Jaroslaw, B., S. Barbara, and J. Patryk, *The comparison of low-velocity impact resistance of aluminum/carbon and glass fiber metal laminates.* Polymer Composites, 2016. **37**(4): p. 1056-1063.

[7] Gonzalez-Canche, N.G., E.A. Flores-Johnson, and J.G. Carrillo, *Mechanical characterization of fiber metal laminate based on aramid fiber reinforced polypropylene.* Composite Structures, 2017. **172**: p. 259-266.

[8] Sharma, A.P., et al., *Effect of through thickness metal layer distribution on the low velocity impact response of fiber metal laminates.* Polymer Testing, 2018. **65**: p. 301-312.

[9] Asundi, A. and A.Y.N. Choi, *Fiber metal laminates: An advanced material for future aircraft.* Journal of Materials Processing Technology, 1997. **63**(1–3): p. 384-394.

[10] Huda, Z., T. Zaharinie, and G.J. Min, *Temperature Effects on Material Behavior of Aerospace Aluminum Alloys for Subsonic and Supersonic Aircraft.* Journal of Aerospace Engineering, 2010. **23**(2).

[11] Wu, H.F., *Effect of temperature and strain rate on tensile mechanical properties of ARALL-1 laminates.* Journal of Materials Science, 1991. **26**(14): p. 3721-3729.

[12] Wu, H.F., *Temperature dependence of the tensile behaviour of aramid/aluminium laminates.* Journal of Materials Science, 1993. **28**(1): p. 19-34.

[13] Badawy, A.A.M., *Impact behavior of glass fibers reinforced composite laminates at different temperatures.* Ain Shams Engineering Journal, 2012. **3**(2): p. 105-111.

[14] Hu, Y., et al., *The effects of temperature variation on mechanical behaviors of polyetheretherketone-based fiber metal laminates.* Polymer Composites, 2016.

[15] Hawileh, R.A., et al., *Temperature effect on the mechanical properties of carbon, glass and carbon–glass FRP laminates.* Construction and Building Materials, 2015. **75**: p. 342-348.

[16] Jakubczak, P. and J. Bieniaś, *Comparison of quasi static indentation and dynamic loads of glass and carbon fibre aluminium laminates*. Vol. 88. 2016. 404-410.

[17] Mahieux, C.A., K.L. Reifsnider, and S.W. Case, *Property Modeling across Transition Temperatures in PMC's: Part I. Tensile Properties.* Applied Composite Materials, 2001. **8**(4): p. 217-234.

[18] Gibson, A.G., et al., *Laminate Theory Analysis of Composites under Load in Fire.* Journal of Composite Materials, 2005. **40**(7): p. 639-658.

[19] Correia, J.R., et al., *Mechanical behaviour of pultruded glass fibre reinforced polymer composites at elevated temperature: Experiments and model assessment.* Composite Structures, 2013. **98**: p. 303-313.

[20] Wong, K.J., *Moisture absorption characteristics and effects on mechanical behaviour of carbon/epoxy composite : application to bonded patch repairs of composite structures*. 2013, Université de Bourgogne.

* For correspondence; Tel. + (60) 163026502, E-mail: zhenpei.chow@gmail.com

* For correspondence; Tel. + (60) 75557072, E-mail: azaini@mail.fkm.utm.my